Accelerated Prediction of Photon Transport in Nanoparticle Media Using Machine Learning Trained With Monte Carlo Simulations

Daniel Carne
School of Mechanical Engineering and
Birck Nanotechnology Center,
Purdue University,
West Lafayette, IN 47907

Joseph Peoples
School of Mechanical Engineering and
Birck Nanotechnology Center,
Purdue University,
West Lafayette, IN 47907

Dudong Feng
School of Mechanical Engineering and
Birck Nanotechnology Center,
Purdue University,
West Lafayette, IN 47907

Xiulin Ruan[1]
School of Mechanical Engineering and
Birck Nanotechnology Center,
Purdue University,
West Lafayette, IN 47907
e-mail: ruan@purdue.edu

Monte Carlo simulations for photon transport are commonly used to predict the spectral response, including reflectance, absorptance, and transmittance in nanoparticle laden media, while the computational cost could be high. In this study, we demonstrate a general purpose fully connected neural network approach, trained with Monte Carlo simulations, to accurately predict the spectral response while dramatically accelerating the computational speed. Monte Carlo simulations are first used to generate a training set with a wide range of optical properties covering dielectrics, semiconductors, and metals. Each input is normalized, with the scattering and absorption coefficients normalized on a logarithmic scale to accelerate the training process and reduce error. A deep neural network with ReLU activation is trained on this dataset with the optical properties and medium thickness as the inputs, and diffuse reflectance, absorptance, and transmittance as the outputs. The neural network is validated on a validation set with randomized optical properties, as well as nanoparticle medium examples including barium sulfate, aluminum, and silicon. The error in the spectral response predictions is within 1% which is sufficient for many applications, while the speedup is 1–3 orders of magnitude. This machine learning accelerated approach can allow for high throughput screening, optimization, or real-time monitoring of nanoparticle media's spectral response. [DOI: 10.1115/1.4062188]

Keywords: machine learning, artificial neural network, radiative heat transfer, Monte Carlo, nanoparticle media

Introduction

Photon transport simulations in scattering media are used in a wide variety of applications from thermal radiative transport to biomedical engineering. Typically for nanoparticle media, Mie theory or numerical methods are used to calculate the scattering and absorption properties of individual particles, which are then used in Monte Carlo simulations to predict the spectral response [1]. Monte Carlo simulations were introduced for radiative heat transfer by Howell and Perlmutter in 1964 [2] and has since been used by many other researchers to solve radiative heat transfer problems. Recent examples include radiative cooling coatings [3,4] and protective systems for spacecraft [5]. Meanwhile, several open-source Monte Carlo programs have been published [6,7]. One such program, Monte Carlo for multi-layer media (MCML) by Wang et al. was originally created for photon transport in multilayered tissues [7] but has also been utilized for radiative cooling [3,4]. Several other Monte Carlo programs have shown the speedup provided from parallel processing is equivalent to the number of processors used [8]. A similar Monte Carlo program to MCML, written by Alerstam et al., targets Nvidia Graphics Processing Units (GPUs) to reduce the necessary computational time [9]. This approach provides up to 1000 times speedup over traditional central processing unit (CPU) based programs. Even with these advancements and parallel processing techniques, Monte Carlo simulations can still take up to an hour for certain applications such as radiative cooling coatings. Further improvements are necessary to allow for high throughput screening and certain optimization methods.

Most recently, machine learning techniques, trained with rigorous simulation or experimental data, are frequently used to significantly accelerate computational predictions. This approach has been successfully applied to simulations in many different fields of transport phenomena such as molecular dynamics [10], computational fluid dynamics [11], and heat transfer [12,13] including a review paper going over many of these methods and their applications [14]. Machine learning has also been applied to photon Monte Carlo simulations. Peng et al. achieved a 76-fold speedup by using a convolutional neural network to reduce noise in radiation therapy dosing maps created by Monte Carlo simulations [15]. Hokr and Bixler trained a fully connected neural network with GPU-based Monte Carlo simulations to predict the optical properties of single-layer homogenous tissue, commonly referred to as the inverse problem [16]. Some researchers have developed machine learning models to predict dose maps for radiation therapy patients, directly replacing Monte Carlo simulations to predict where particles are absorbed [17,18]. To our knowledge, machine learning methods to predict general spectral optical responses of particle composite media, including reflection, transmission, and absorption have not yet been applied.

In this study, we demonstrate a fully connected neural network to predict the reflectance, transmittance, and absorptance of nanoparticle composite media, with a broad range of optical properties for applications across many different materials. First, the neural network is trained with Monte Carlo simulations that provide the spectral response over a large range of randomized optical properties including the refractive index, scattering coefficient, absorption coefficient, and asymmetry parameter. Then, the optical properties and medium thickness are provided as the inputs to the neural network, with the diffuse reflectance, absorptance, and transmittance as the outputs. Subsequently, to test the neural network's capabilities and accuracy, the spectral response of three nanoparticle coatings of $BaSO_4$, Si, and Al are examined in further detail representing a dielectric, semiconductor, and metal , respectively. Mie theory and effective medium theory are used to calculate the

[1]Corresponding author.

Contributed by the Heat Transfer Division of ASME for publication in the Journal of Heat and Mass Transfer. Manuscript received August 1, 2022; final manuscript received March 20, 2023; published online April 11, 2023. Assoc. Editor: Xianfan Xu.

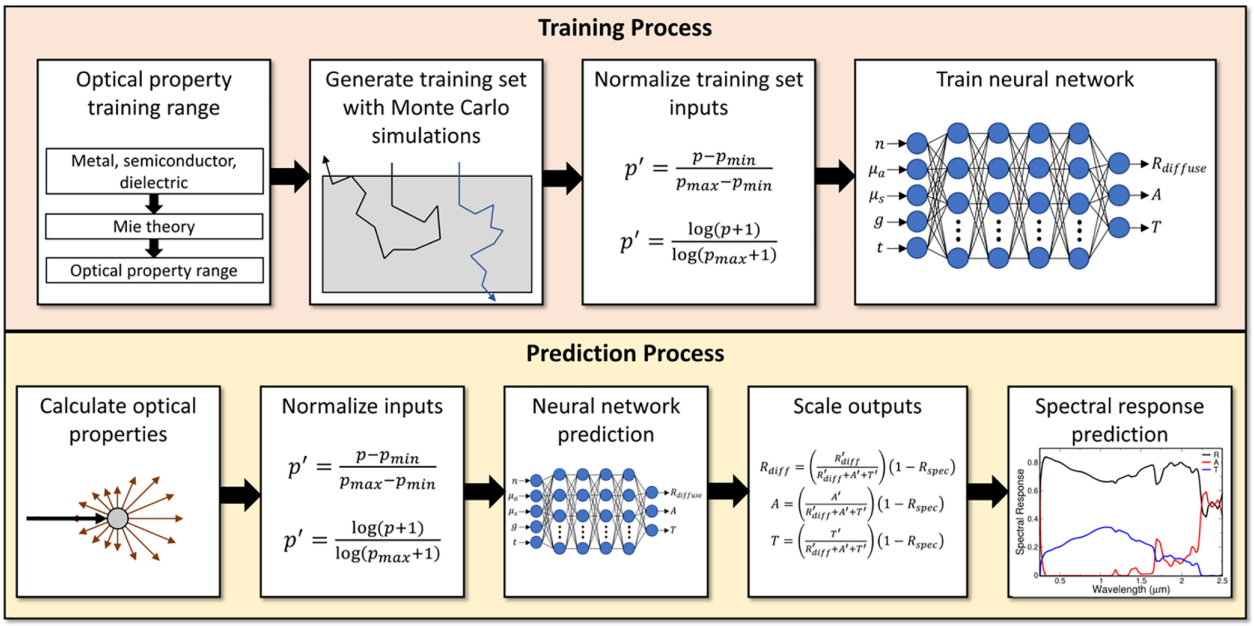

Fig. 1 Training and prediction processes; the training process including assessing the optical property range to train on, generating the training set with Monte Carlo simulations, normalizing the input values, and training the neural network. The prediction process includes calculation of the optical properties, normalizing the input values, neural network prediction, and output scaling to determine the spectral response prediction.

scattering coefficient, absorption coefficient, and asymmetry parameter of each medium across the solar spectrum, then the neural network's predictions will be compared to rigorous Monte Carlo simulations.

Methodology

This study will focus on nanoparticle media that can be approximated as effective homogeneous scattering media. For nanoparticle media, Mie theory is used to calculate the optical properties of a single particle, including the absorption coefficient, scattering coefficient, and asymmetry parameter from known refractive indices and extinction coefficients at varying wavelengths. These values are then volume averaged with the medium the particles are embedded in to create an effective homogenous scattering medium. Once these values are known, typically Monte Carlo simulations solve for specular reflection, diffuse reflection, absorption, transmission, and the location within the medium where photons are absorbed. For our purposes, a deep neural network is trained to predict diffuse reflection, absorption, and transmission, directly replacing Monte Carlo simulations. The specular reflection is easily analytically calculated so this is not necessary to predict with the neural network. The location of absorption within the medium is not considered in this research as the quantities of interest for heat transfer applications are the spectral reflectance, transmittance, and absorptance. This process is visualized in Fig. 1 for both the training process and prediction process, and each method is described in further detail below.

Mie Theory. Mie theory is an analytical solution to Maxwell's equations for electromagnetic wave scattering on an individual particle with a diameter comparable to the wavelength of light. First, Mie theory is applied to calculate the scattering efficiency (Q_{sca}), absorption efficiency (Q_{abs}), and asymmetry parameter (g) of individual particles [19–21]. The asymmetry parameter is defined as the integral over the cosine weighted phase function, where 1 indicates entirely forward scattering and 0 indicates isotropic forward and backward scattering. These values could also be calculated by numerical methods for particles with irregular shapes. Subsequently, the nanoparticle medium is approximated as an effective homogeneous scattering medium, whose scattering coefficient, absorption coefficient, and asymmetry parameter are calculated based on the optical properties of individual particles of different size together with their volume fractions [4].

Monte Carlo Photon Transport. For this study, a custom parallel Monte Carlo simulation code is used to calculate spectral responses for the neural network to train on. The code is based on the MCML program by Wang et al. [7], where additional details can be found. For photons interacting with a medium, there are four possible outcomes: specular reflection, diffuse reflection, transmission, or absorption. Initially, the specular reflectance is calculated by

$$R_{spec} = \left(\frac{n_1 - n_2}{n_1 + n_2}\right)^2 \tag{1}$$

where n_1 is the index of refraction of the ambient medium, often air, and n_2 is the index of refraction of the medium being calculated [22]. The diffuse reflection, absorption, and transmission are calculated with the Monte Carlo simulation using 30,000 photon packets each. Sampling 20 Monte Carlo simulations across 300 varying sets of optical properties, the average sample standard deviation for the spectral response is 0.0023.

Radiative Properties in the Solar Spectrum. This work largely focuses on the radiative properties of nanoparticle media under solar irradiation. To calculate the solar reflectance for surfaces on the earth, the solar irradiation at normal air mass 1.5 is used [23]. Only solar irradiation between 0.25 and 2.5 μm is considered here as irradiation outside this spectrum is negligible. The solar reflectance can be calculated by

$$R_{solar} = \frac{\int_{\lambda_1}^{\lambda_2} R_\lambda G_\lambda d\lambda}{\int_{\lambda_1}^{\lambda_2} G_\lambda d\lambda} \tag{2}$$

where R_λ is the medium's spectral reflectance and G_λ is the spectral solar irradiation.

Table 1 Range of different optical properties included in the dataset

Optical property	Range	Distribution
Refractive index	1–10	Linear
Absorption coefficient (cm^{-1})	0–1,000,000	Logarithmic
Scattering coefficient (cm^{-1})	0–150,000	Logarithmic
Asymmetry parameter	0–1	Linear
Medium thickness (μm)	5–500	Linear

Neural Network. Neural networks are commonly used for regression problems, mapping the relationship between the inputs and the outputs. This study utilizes a fully connected neural network with four hidden layers, five inputs, and three outputs as shown in Fig. 1. The five inputs, the same as the inputs to the Monte Carlo simulation, are the refractive index, absorption coefficient, scattering coefficient, asymmetry parameter, and thickness of the medium.

The ReLu activation function is chosen as it is a standard activation function for regression problems, given by

$$z = \begin{pmatrix} 0 & \text{if} & n < 0 \\ n & \text{if} & n \geq 0 \end{pmatrix} \tag{3}$$

where z is the output of a node and n is the input. This activation function is applied to every node except in the output layer, where a linear activation function is used [24]. The loss function used is the mean square error, given by

$$\text{MSE} = \frac{1}{N}\sum_{i=1}^{N}(y_i - \hat{y}_i)^2 \tag{4}$$

where N is the number of training points per batch, y_i is the true value, and $\hat{y}_i$ is the predicted value. The back propagation stochastic gradient descent uses the ADAM optimization method with a learning rate of 0.001 to decrease the required number of epochs [25]. The number of hidden layers and nodes in each layer are slowly increased until decreases in the MSE cease, providing a neural network with four hidden layers consisting of 2000, 2000, 20, and 10 nodes in each respective layer. While this configuration provided the lowest error, the majority of the architectures tested provided similarly low error as long as there were a sufficient total number of nodes. Further optimization could be used to decrease the number of nodes used.

To increase training speed and solution quality, each input is normalized before training [26]. The refractive index, asymmetry parameter, and thickness are normalized by

$$p' = \frac{p - p_{\min}}{p_{\max} - p_{\min}} \tag{5}$$

where p represents each individual input to the neural network [27]. With prior knowledge of how the absorption and scattering coefficients affect the spectral response, they are normalized on a logarithmic scale by

$$p' = \frac{\log(p+1)}{\log(p_{\max}+1)} \tag{6}$$

Due to errors in the neural network, outputs may sum up to values other than one which would violate the following relation

$$1 = R_{\text{spec}} + R_{\text{diff}} + A + T \tag{7}$$

To prevent an unphysical solution and enforce Eq. 7, as well as to adjust for the previously calculated specular reflectance, the output predictions of the neural network are normalized by

$$R_{\text{diff}} = \left(\frac{R'_{\text{diff}}}{R'_{\text{diff}} + A' + T'}\right)(1 - R_{\text{spec}}) \tag{8}$$

$$A = \left(\frac{A'}{R'_{\text{diff}} + A' + T'}\right)(1 - R_{\text{spec}}) \tag{9}$$

$$T = \left(\frac{T'}{R'_{\text{diff}} + A' + T'}\right)(1 - R_{\text{spec}}) \tag{10}$$

where R'_{diff}, A', and T' are the neural network outputs before normalization. The neural network training process requires 11.5 min to run 100 epochs where additional epochs do not significantly decrease error.

Data Set. A dataset of 41,000 sets of randomly sampled optical properties and their respective spectral response is generated by the Monte Carlo simulation described above with 30,000 incident photon packets each. The optical properties used in this dataset cover a broad range, as shown in Table 1, to allow for predictions across many different potential medium types. At small scattering and absorption coefficients, slight changes can significantly impact the spectral response. As these coefficients increase, the change in the spectral response levels off. To reduce the number of data points necessary, as well as to properly model low scattering and absorption coefficients, these values will be randomly sampled from a logarithmic scale. The dataset is split so that 97.5% is used to train the neural network while 2.5% is used as the validation set. While these data do not reflect any specific medium's optical properties, the goal is to completely map the domain so that any possible set of optical properties can be predicted. Further validation will be performed with optical inputs from real nanoparticle media. Creating this dataset with Monte Carlo simulations in parallel took approximately 16 h using ten nodes with two Dell Rome CPUs each.

Results and Discussion

Results of the trained neural network's photon transport predictions are shown in Fig. 2 for each spectral response. The

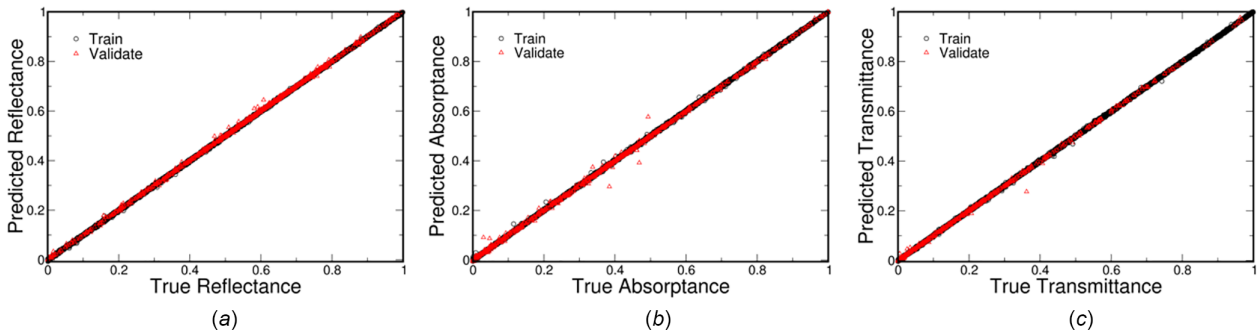

Fig. 2 Neural network predicted value versus the true value for: (*a*) reflectance, (*b*) absorptance, and (*c*) transmittance

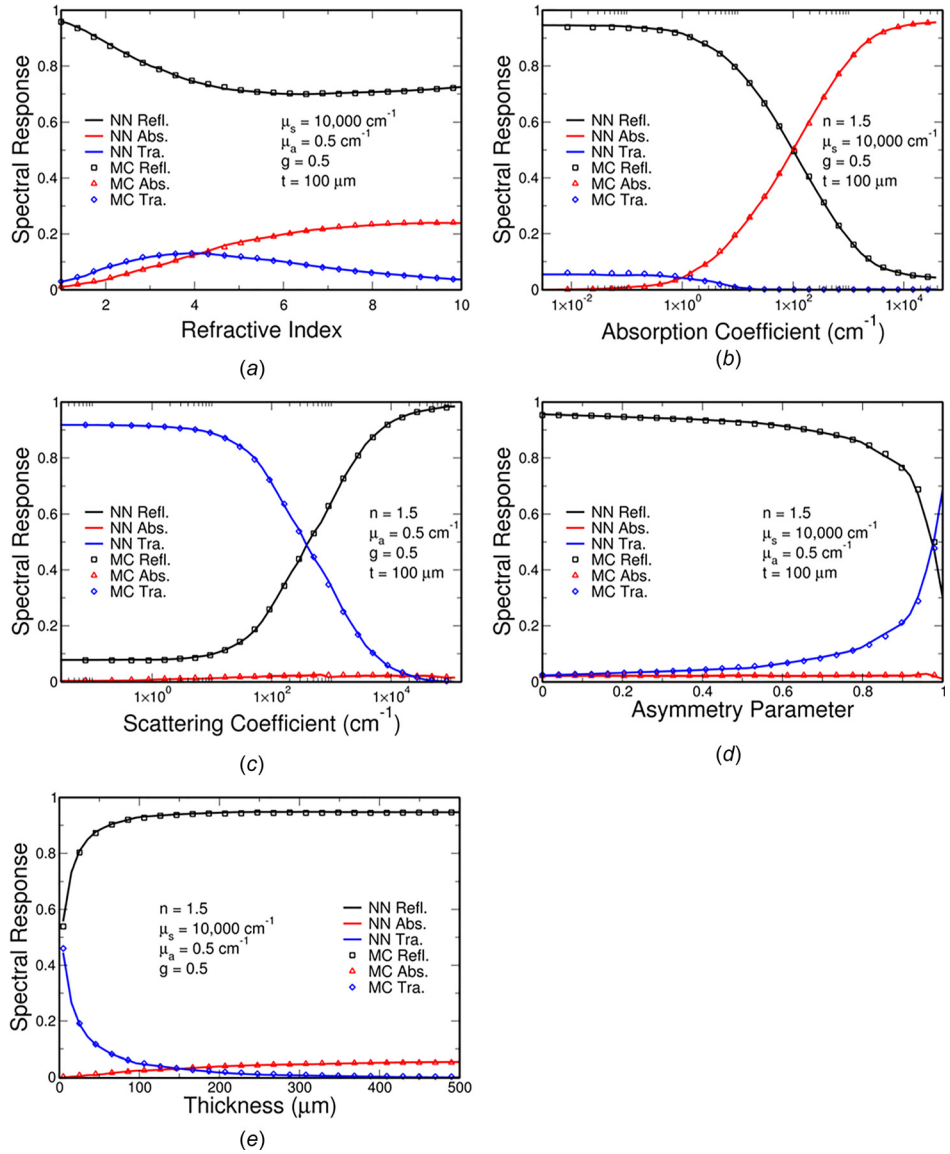

Fig. 3 Neural network predictions and Monte Carlo spectral responses varying the: (*a*) refractive index, (*b*) absorption coefficient, (*c*) scattering coefficient, (*d*) asymmetry parameter, and (*e*) thickness. All other parameters held constant at $n = 1.5$, $\mu_a = 0.5\,\text{cm}^{-1}$, $\mu_s = 10,000\,\text{cm}^{-1}$, $g = 0.5$, $t = 100\,\mu\text{m}$.

average absolute error of the training and validation sets is 0.0014 and 0.0025, respectively. This error is small and generally negligible for many applications, however a very small percentage of data points in the validation set saw significant error up to 0.15. Errors this large are only seen when an input to the neural network is near the upper of lower bound of the training set range. For example, the maximum error of 0.15 had an asymmetry parameter of 0.9995, extremely close to the upper bound of one. This is important to note that in the final design evaluations, the selected neural network prediction should still be validated against Monte Carlo simulations.

Figure 3 shows the spectral response results comparison when varying a single input parameter while fixing others. The fixed properties were chosen to allow significant variation in the spectral response as a single property is varied. Due to the stochastic process and number of photon packets used in the Monte Carlo simulations, there is slight noise in the data provided to the neural network as seen in the plots. The neural network was generally able to average out this noise and not overfit the data provided, meaning the true average error of the neural network predictions may be less than the error as compared to Monte Carlo simulations with a comparable number of photon packets as the training set.

As the training and validation datasets are generated from randomly sampled properties, they are not representative of any specific real materials. To further validate this method and understand the uncertainties involved, barium sulfate, silicon, and aluminum nanoparticle composite media are examined, which, respectively, represent a dielectric, semiconductor, and metal. Each of these materials is expected to have unique spectral responses. Aluminum, a metal, has no electronic band gap often resulting in large absorption coefficients in the solar spectrum. Silicon, a semiconductor, has a moderate electronic bandgap where only high energy photons with energy above the band gap can be readily absorbed. Barium sulfate, a dielectric, has a large electronic band gap preventing the high energy photons within the majority of the solar spectrum from being freely absorbed.

Barium sulfate has become popular as a radiative cooling nanoparticle in paints and films. The reflectance of $BaSO_4$-acrylic paint with a 60% fill fraction of 400 nm diameter particles is calculated at four different common paint thicknesses with the neural network. Here, we see high reflectance due to the combination of large scattering coefficients due to the large refractive index, and near zero absorption in the solar spectrum

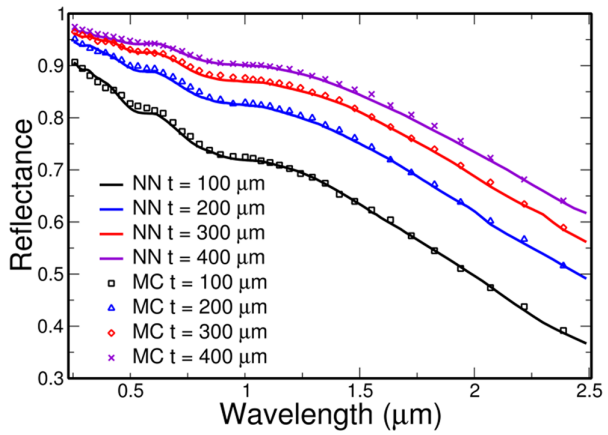

Fig. 4 Neural network and Monte Carlo predictions of $BaSO_4$ reflectance at four different paint thicknesses

Table 2 Monte Carlo and neural network predictions of solar reflectance at different paint thicknesses

	$BaSO_4$ paint thickness			
	100 μm	200 μm	300 μm	400 μm
Monte Carlo	0.7551	0.8473	0.8881	0.9111
Neural network	0.7503	0.8421	0.8843	0.9081
Absolute error	0.0048	0.0052	0.0038	0.003
Relative error	0.64%	0.61%	0.43%	0.33%
Speedup	356×	706×	1189×	1545×

due to the large electronic band gap. The spectral reflectance across the solar spectrum is compared in Fig. 4 between the Monte Carlo simulations and the neural network. Table 2 details the solar reflectance between each thickness paint, where the average relative error is 0.5%, and the maximum absolute difference between the two methods is 0.0052. The neural network tends to provide values within a certain difference of the Monte Carlo simulations, so although the percent error increases as reflectance decreases, the absolute error remains similar. Table 2 also includes the speedup for each paint thickness ranging from 356 to 1545-fold depending on the thickness. At smaller thicknesses, fewer photon packets take fewer steps on average to be reflected or transmitted in the Monte Carlo simulation. This is why the speedup increases as the thickness increases. As the coating thickness increases further, fewer photon packets will reach the lower boundary where they can be transmitted, so the speedup will level off to a constant value. It is also important to note that for every case in this study, both the neural network and Monte Carlo methods were run in the same programing language on an eight-core desktop processor in parallel.

Table 3 Monte Carlo and neural network solar reflectance predictions for aluminum and silicon nanoparticle coatings

	Aluminum	Silicon
Monte Carlo	0.2087	0.4549
Neural network	0.2070	0.4540
Absolute error	0.0017	0.0009
Relative error	0.81%	0.20%

Speedups will vary based on each computer's cooling capacity and number of cores.

The same analysis is performed for 1 μm diameter aluminum particles and 2 μm diameter silicon particles at a 10% fill fraction suspended in air at a total thickness of 50 μm. Figure 5 shows the spectral response for each material, and Table 3 shows the solar reflectance, absolute error, and relative error. In the aluminum, we see significant absorption due to free electron absorption of photons and zero transmission at this thickness. In silicon, within the solar spectrum we see zero absorption below the band gap and increased absorption above the band gap, as expected. A similar trend of agreement between the neural network and Monte Carlo predictions with $BaSO_4$ is seen, here, with aluminum showing a higher relative error in the solar reflectance than the other materials due to its lower reflectance. The solar reflectance absolute error between the two methods here is lower than that of the barium sulfate. This is likely due to barium sulfate having an absorption coefficient near zero which is at the boundary of the training dataset, while silicon and aluminum have nonzero absorption coefficients.

For the aluminum coating, the neural network took 0.057 s while the Monte Carlo simulation took 8.1 s, providing a 162-fold speedup. For the silicon coating, the neural network took 0.17 s while the Monte Carlo simulation took 8.8 s, providing a 52-fold speedup. As the neural network takes the same amount of time to predict the spectral response at each wavelength, the speedup seen is completely dependent on the number of steps a photon packet must take to be reflected, transmitted, or completely absorbed. For materials like barium sulfate with high scattering coefficients, low asymmetry parameters, and low absorption coefficients, the photon packets will take significantly more steps. The aluminum coating here has a lower speedup than seen in the barium sulfate due to the high absorption coefficient, allowing the photon packets to be quickly absorbed without a large number of steps. The silicon coating has an even lower speedup than the aluminum due to the combination of significant absorption of high energy photons, and transmission of low energy photons. With these factors considered, the largest speedups will be realized in materials with high diffuse reflectance and low absorption. Smaller speedups will be seen in materials with high absorption or transmission.

To highlight the acceleration of this method, a high throughput screening example is performed on the nanoparticle size's effect on BaSO4-acrylic paint at a 400 μm thickness with a 60% fill fraction.

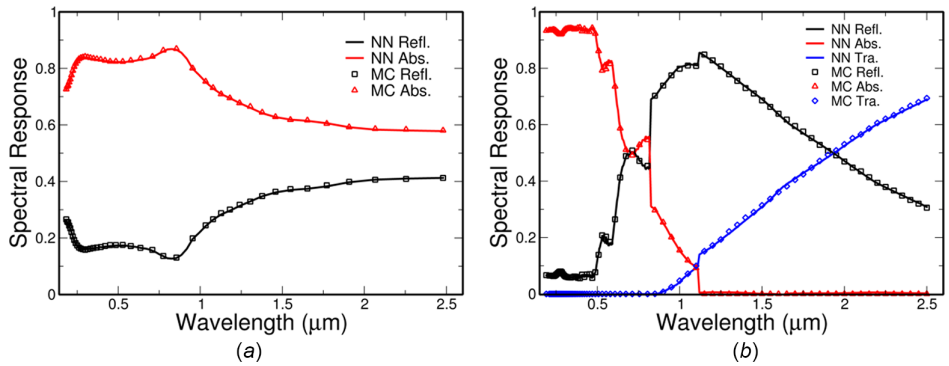

Fig. 5 Spectral response of (*a*) aluminum and (*b*) silicon nanoparticle coatings

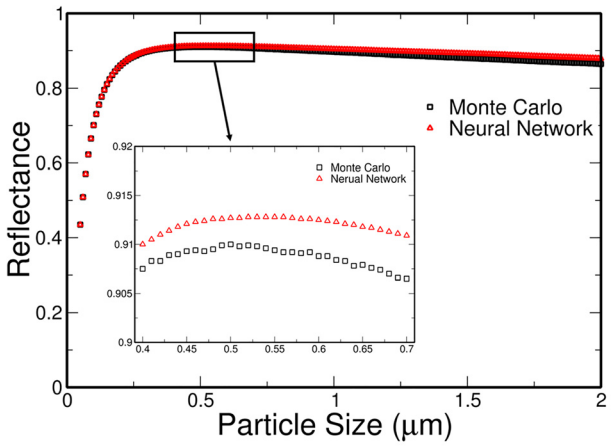

Fig. 6 Monte Carlo and neural network predictions of solar reflectance for varying nanoparticle diameters from 50 to 2000 nm for 400 μm thick $BaSO_4$-acrylic paint with a 60% fill fraction

Particle sizes ranging from 50 to 2000 nm are simulated in 10 nm intervals. The neural network predicts the spectral response of all 196 nanoparticle sizes in 33 s, while the Monte Carlo simulations takes 332 min, providing a 604-fold speedup. Figure 6 shows the solar reflectance near the peak particle sizes from 400 to 700 nm. While the neural network predicts on average 0.84% higher solar reflectance, the overall trend is the same with the optimal particle range around 500 nm to maximize solar reflectance.

The neural network is trained on the values of the spectral response, but it is never directly trained that the summation of each spectral response should be one. Figure 7 shows the absolute error of the silicon nanoparticle coating between the neural network predictions and the Monte Carlo simulations. The summation error of the spectral response is considerably less than the error in each individual spectral response. Neural networks are known for averaging out the error for an individual node, however this being for three separate nodes, the neural network may have learned during the training process that the summation should equal one. This is interesting to note as it shows the neural network could learn a physical aspect of the problem that it was not explicitly trained on, i.e., the summation should be one. This is an advantage of using multitask learning, where all three nodes are outputs of one neural network instead of three different neural networks predicting each value. To calculate the spectral response, only two of the values are needed, as the third could be calculated using the summation rule. This approach is commonly used in spectrometry where the reflectance and transmittance are measured, and the remaining photons are assumed to be absorbed. The neural network benefits from outputting all three values, as the error is averaged between the three outputs so that the summation is one.

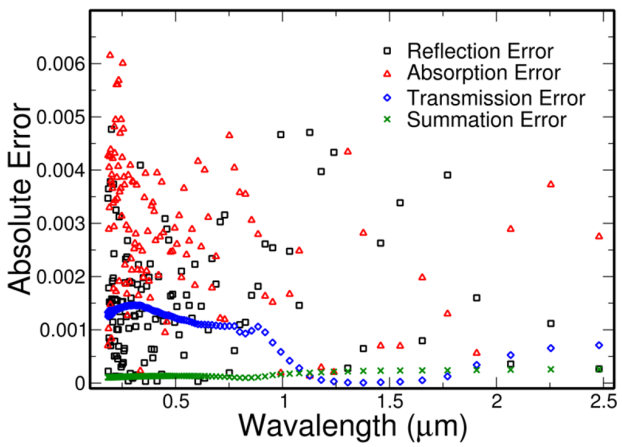

Fig. 7 Absolute error of each spectral response and the spectral response summation between the neural network predictions and Monte Carlo simulations for a silicon nanoparticle coating

Conclusion

In summary, this study demonstrates a fully connected deep neural network can significantly accelerate diffuse reflectance, absorptance, and transmittance predictions in nanoparticle media typically calculated by Monte Carlo simulations. A dataset of 41,000 examples with randomly sampled material properties is generated with Monte Carlo simulations for the neural network to train on. This dataset includes a wide range of optical properties to cover many potential materials including dielectrics, semiconductors, and metals. After training, the neural network predictions show little deviation from the Monte Carlo simulations. This method is further validated with three different nanoparticle media, barium sulfate, silicon, and aluminum. Analysis of these materials shows consistent results with negligible differences between the neural network predictions and the Monte Carlo simulations with error less than 1%. Results also show the error in the summation of the spectral response is considerably lower than the error in each individual spectral response. This may indicate the neural network learning a physical aspect of this problem that it was not explicitly trained on, that the summation of a spectral response is equal to one. Depending on the material, medium thickness, and number of photon packets, significant speedups can be achieved up to 1–3 orders of magnitude. For the barium sulfate radiative cooling paint test, speedups between 356- and 1545-fold are seen at the thicknesses tested. A high throughput example of varying nanoparticle size in $BaSO_4$-acrylic paint shows the neural network provides a 604-fold speedup while finding a similar optimal particle size as the Monte Carlo simulations to maximize solar reflectance. This machine learning approach can provide many exciting new possibilities by rapidly simulating radiative cooling or heating, allowing for high throughput material screening, complex multiparticle optimization methods, and real-time monitoring.

Declaration of Competing Interest

The authors declare no competing interest with the work presented.

Authorship Contribution Statement. Daniel Carne: Methodology, Investigation, Data Acquisition, Writing – original draft, Writing – review & editing. Joseph Peoples: Methodology, Writing – review & editing. Dudong Feng: Methodology, Writing – review & editing. Xiulin Ruan: Conceptualization, Funding Acquisition, Supervision, Writing – review & editing.

Acknowledgment

D.C., D.F., and X.R. acknowledge partial support from the U.S. National Science Foundation (Award No. 2102645). J.P. acknowledges support from the NASA Space Technology Graduate Research Opportunity Program (Grant No. 80NSSC20K1187).

Data Availability Statement

The datasets generated and supporting the findings of this article are obtainable from the corresponding author upon reasonable request.

Funding Data

- Division of Materials Research (Award No. 2102645; Funder ID: 10.13039/100000078).
- National Aeronautics and Space Administration (Award No. 80NSSC20K1187; Funder ID: 10.13039/100000104).

References

[1] Frisvad, J. R., Christensen, N. J., and Jensen, H. W., 2007, "Computing the Scattering Properties of Participating Media Using Lorenz-Mie Theory," ACM Trans. Graph., **26**(3), p. 60.

[2] Howell, J. R., and Perlmutter, M., 1964, "Monte Carlo Solution of Thermal Transfer Through Radiant Media Between Gray Walls," ASME J. Heat Mass Transfer-Trans. ASME, **86**(1), pp. 116–122.

[3] Li, X., Peoples, J., Yao, P., and Ruan, X., 2021, "Ultra-White BaSO4 Paint and Film With Remarkable Radiative Cooling Performance," ACS Appl. Mater. Interfaces, **13**(18), pp. 21733–21739.

[4] Peoples, J., Li, X., Lv, Y., Qiu, J., Huang, Z., and Ruan, X., 2019, "A Strategy of Hierarchical Particle Sizes in Nanoparticle Composite for Enhancing Solar Reflection," Int. J. Heat Mass Transfer, **131**, pp. 487–494.

[5] Vuolo, M., Giraudo, M., Musenich, R., Calvelli, V., Ambroglini, F., Burger, W. J., and Battiston, R., 2016, "Monte Carlo Simulations for the Space Radiation Superconducting Shield Project (SR2S)," Life Sci. Space Res., **8**, pp. 22–29.

[6] Prahl, S. A., 1989, "A Monte Carlo Model of Light Propagation in Tissue," Proc. SPIE **10305**, p. 1030509.

[7] Wang, L., Jacques, S. L., and Zheng, L., 1995, "MCML-Monte Carlo Modeling of Light Transport in Multi-Layered Tissues," Comput. Methods Programs Biomed., **47**(2), pp. 131–146.

[8] Hollow, J. R., 1998, "The Monte Carlo Method in Radiative Heat Transfer," ASME J. Heat Mass Transfer-Trans. ASME, **120**(3), pp. 547–560.

[9] Alerstam, E., Svensson, T., and Andersson-Engels, S., 2008, "Parallel Computing With Graphics Processing Units for High-Speed Monte Carlo Simulation of Photon Migration," J. Biomed. Opt., **13**(6), p. 060504.

[10] Botu, V., and Ramprasad, R., 2015, "Adaptive Machine Learning Framework to Accelerate Ab Initio Molecular Dynamics," Int. J. Quantum Chem., **115**, pp. 1074–1083.

[11] Maulik, R., San, O., Rasheed, A., and Vedula, P., 2019, "Subgrid Modelling for Two-Dimensional Turbulence Using Neural Networks," J. Fluid Mech., **858**, pp. 122–144.

[12] Chowdhury, P. R., and Ruan, X., 2022, "Unexpected Thermal Conductivity Enhancement in Aperiodic Superlattices Discovered Using Active Machine Learning," NPJ Comput. Mater, **8**(12), p. 12.

[13] Wei, H., Bao, H., and Ruan, X., 2020, "Machine Learning Prediction of Thermal Transport in Porous Media With Physics-Based Descriptors," Int. J. Heat Mass Transfer, **160**, p. 120176.

[14] Wei, H., Bao, H., and Ruan, X., 2022, "Perspective: Predicting and Optimizing Thermal Transport Properties With Machine Learning Methods," Energy AI, **8**, p. 1000153.

[15] Peng, Z., Shan, H., Liu, T., Pei, X., Wang, G., and Xu, X. G., 2019, "A Denoising Convolutional Neural Network to Accelerate Monte Carlo Radiation Transport Simulations: A Proof of Principle With Patient Dose From X-Ray CT Imaging," IEEE Access, **7**, pp. 76680–76689.

[16] Hokr, B. H., and Bixler, J. N., 2021, "Machine Learning Estimation of Tissue Optical Properties," Sci. Rep., **11**, p. 6561.

[17] Lee, M. S., Hwang, D., Kim, J. H., and Lee, J. S., 2019, "Deep-Dose: A Voxel Dose Estimation Method Using Deep Convolutional Neural Network for Personalized Internal Dosimetry," Sci. Rep., **9**(1), p. 10308.

[18] Keal, J., Santos, A., and Douglass, M., 2021, "Radiation Dose Calculation in 3D Heterogeneous Media Using Artificial Neural Networks," Med. Phys., **48**(5), pp. 2636–2645.

[19] Huang, Z., and Ruan, X., 2017, "Nanoparticle Embedded Double-Layer Coating for Daytime Radiative Cooling," Int. J. Heat Mass Transfer, **104**, pp. 890–896.

[20] Bohren, C. F., and Huffman, D. R., 2008, *Absorbing and Scattering of Light by Small Particles*, Wiley, Weinheim, Germany.

[21] Modest, M. H., and Azad, F. H., 1980, "The Influence and Treatment of Mie-Anisotropic Scattering in Radiative Heat Transfer," ASME J. Heat Mass Transfer-Trans. ASME, **102**(1), pp. 92–98.

[22] Pedrotti, F. L., Pedrotti, L. M., and Pedrotti, L. S., 2017, *Introduction to Optics*, Cambridge University Press, Cambridge, UK..

[23] ASTM G173-03, 2020, "Standard Tables for Reference Solar Spectral Irradiances: Direct Normal and Hemispherical on 37° Tilted Surface," Book of Standards, Vol. 14.04.

[24] Sharma, S., Sharma, S., and Athaiya, A., 2020, "Activation Functions in Neural Networks," Int. J. Appl. Sci. Technol, **4**(12), pp. 310–316.

[25] Kingma, D. P., and Ba, J., 2014, "Adam: A Method for Stochastic Gradient Descent," arXiv:1412.6980.

[26] Sola, J., and Sevilla, J., 1997, "Importance of Input Data Normalization for the Application of Neural Networks to Complex Industrial Problems," IEEE Trans. Nucl. Sci., **44**(3), pp. 1464–1468.

[27] Kim, D., 1999, "Normalization Methods for Input and Output Vectors in Backpropagation Neural Networks," Int. J. Comput. Math., **71**(2), pp. 161–171.